ACI STRUCTUAL JOURNAL TECHINICAL PAPER
Title no. 98-S34

Bond Behavior between Fiber-Reinforced Polymer Laminates and Concrete

by Kasumassa Nakaba, Toshiyuki Kanakubo, Tomoki Furuta, and Hiroyuki Yoshizawa

This research examines the bond behavior between fiber-reinforced polymer (FRP) laminates and concrete. To obtain the local bond stress versus slippage relationship, a double-face shear type bond test is conducted. The primary test variables are the types of fiber and concrete. The test results show that fiber stiffness influences both the bond strength and shape of stress distribution. The obtained local bond stress - slip relationships, however, are not influenced by the type of fiber. Only the maximum local bond stress increases as concrete compressive strength also increases. A new model representing the local bond stress versus slippage relationship is proposed using Popovics's formula, which has been adapted to present the concrete compressive stress-strain relationship. A numerical analysis is performed to confirm the model, and experimental results are presented. The analytical results show a good agreement with the bond strength and strain distribution found in the experimental results.

Keywords: bond; fiber reinforcement; local behavior; numerical analysis; polymers; slip; stiffness;

INTRODUCTION

Fiber-reinforced polymers (FRPs) have already been widely used in the aeronautics and space industries, as well as in the sport and recreation industries. The resin in these case, however, is impregnated between the fine fibers beforehand; after they are shaped in the factory, they are heated and made into a laminate - type FRP. When such materials are used in civil engineering applications, it is difficult to heat them at construction sites, so resinless laminates (sheet – type fiber) have been developed which are treated at the work site with a resin that hardens at normal ambient temperatures. Fibers used in retrofitting work have fine fibers aligned in a single direction and are made into thin planes ranging in thickness from 0.1 to 0.4 mm. To improve the bending strength of columns and beams, these sheets are applied in the axial direction of the elements, but they are applied perpendicularly to the axial direction when the goal is to increase shear strength and ductility.

The anchorage between concrete and FRP laminates plays an important role in reinforcing design. As a brittle material, FRP shows a lack of ductility, and the failure mode occurs suddenly without preceding yielding. Recently, many studies have been undertaken to understand the bond behavior between concrete and FRP laminates, but current understanding has not advanced sufficiently to apply FRP laminates, on actual structures. For these reasons, in terms of adhesion, it is necessary to confirm the safety of FRP laminates, or to seek a bond length considered to have an adequately safe bond stress, to prevent the appearance and progress of bond rupture. In cases when the bond rupture or anchorage rupture is unavoidable, it is necessary to obtain the rupture strength experimentally, based on reliable data that adequately consider safety factors.

PREVIOUS RESEARCH

Testing method

Figure 1 shows some specimen types used in the bond test between FRP laminates and concrete. Experiments using a tile or similar methods (Fig.1(a)) to directly obtain the bond strength have been performed. But in terms of bending and shearing in this method, it is difficult to directly estimate the bond characteristics of the concrete-fiber system. One alternative that has been widely used to solve this problem, and was adopted in this research, consists of a prism with a notch at the center, reinforced with FRP laminates on both faces (Fig.1(b)). Similarly, another alternative consisting of two prisms reinforced at the center with FRP laminates (Fig.1(c)) is proposed to estimate the bending. To remove the acting force's eccentricity in experiments using laminates in both faces, experiments using laminate in one face (Fig.1(d)) and laminate inserted in two concrete prisms (designaied Fig.1(e)) have been performed. In this sort of experiment, when the anchorage length is shorter, bond failure with delamination of laminates usually occurs. When the anchorage length is longer, failure occurs with FRP rupture. Also, it is reported that when the anchorage length increases, the failure force tends to be higher, and the apparent average bond stress decreases.

Effective bond length

In a pure tensile experiment, the bond strength at average stress has the tendency to decrease when the bond area increases.This occurs because the bond stress is not distributed throughout the full area of the bond length. It has been reported by previous studies that the bond stress is distributed in the region from the loaded end of the laminate, or from the crack position, with a length not more than 100mm from those points. Previous studies have reported the following results: 75[1], 101, 60[2], 20~90[3], and 40mm[4]. Bond stress distribution obtained from these experiments differs form experiment to experiment, and thus must be carefully considered.

Local bond stress - slip relationship

An important step toward understanding bond behavior is to have an assumption for local bond stress versus slip relationship. Tensile strength in the case of bond failure, strain distribution of FRP, and bond stress distributions can be obtained using bond stress versus slip relationship model by mathematical or numerical analysis. Experiments on

ACI Structural Journal, V98, No.3,May-June 2001.
MS No.00-131 received May 31,2000, and reviewed under Institute publication policies. Pertinent discussion will be published in the March-April 2002 ACI Structural Journal if received by November 1,2001.

Kasumassa Nakaba *is a purchasing engineer at Renault do Brazil S/A, Curitiba City , Parana state, Brazil. He received his civil engineering degree from the Federal University of Paraná, Brazil, and his MS in Engineering form the University of Tsukuba, Japan.His research interests include the Fiber-reinforced polymer systems for concrete structures.*

ACI member **Toshiyuki Kanakubo** *is Assistant professor at the Institute of Engineering Mechanics and Systems at the University of Tsukuba. He received his PhD in engineering from the University of Tsukuba. His research interests include fiber reinforced concrete, fiber-reinforced polymer for concrete, and bond mechanism of concrete structures.*

Tomoki Furuta *is a research engineer in Industrial Mechanical Products Division of Bando Chemical Industries, Ltd., Hyougo, Japan. He received his PhD in engineering from the University of Tokyo, Japan. His research interests include hybrid structures and controlling buildings.*

Hiroyuki Yoshizawa *is a research engineer at Nippon Steel Composite Co., Ltd., Tokyo, Japan. He received his PhD in civil engineering from the Ibaraki University, Japan.*

bond that analyze specimens have been carried out, and the proceedures applied to those experiments are divided in three types, as follows; a) cut off type[3]; b) bilinear type[4]; and c) tensile softening type[5]. Figure 2 shows typical models for these three types.

RESEARCH SIGNIFICANCE AND OBJECTIVE

The main objective of this research is to propose a bond stress- versus-slip model that can provide the effective bond length and the bond strength for externally bonded FRP laminates to concrete. To reach the objective, double-face shear type bond test is conducted. The primary test variables are the types of fiber and concrete. A numerical analysis is also performed to compare the proposed model with experimental results.

Another goal is to address the factors affecting the bond behavior between FRP laminates and concrete. The factors are: stiffness (laminate thickness times elastic modulus), concrete strength, Influence of putty thickness.

EXPERIMENTAL PROGRAM

Specimen

The specimen adopted for this research is shown in Fig. 3. The specimen consists of a concrete prism (100 x 100 x 600mm) cracked at the center using a hammer on the notch after the reinforcing with FRP laminates. The two steel bars also have no connection, which means that the two prisms are connected only through the FRP laminates. The FRP system used in this research consists of fiber impregnated with epoxy resins, with the primarily preparation of the concrete substrate using primer and putty. Putty is a thickened epoxy paste used to fill voids and smooth surface discontinuities.

FRP laminates are bonded at two opposite sides of the specimen. One of the sides of the specimen was reinforced with a confinement FRP allowing the occurrence of delamination of the laminate only on the opposite side, where the strain gages were set. The parameters of the test will be discussed in the following section. Once the tensile force from the FRP is transferred into the concrete, there is nearly no bond stress between the unbonded region. This means that when the bonded length exceeds a critical length (equals effective bond length), the fracture load remains constant. This critical bonded length is smaller than 100mm and the bond length used for this research was set to 300mm. The laminate width exhibited great influence on the bond behavior only when it was less than 10mm[6]. The laminate width chosen for this research was 50mm for all specimens.

The identification of each type of specimen is explained in Fig. 4. Three specimens were made for each combination concrete / mortar - fiber, totaling 36 specimens tested.

Fiber and concrete

Fiber properties are shown in Table 1. The properties of the fibers are values obtained from the manufacturer. Because the main objective of this research is to propose a bond stress-versus- slip model for any combinations of concrete / mortar and FRP in general, carbon (standard and high stiffness) and aramid fiber were used. To verify the influence of the quality of the substrate, the specimens were made by con-

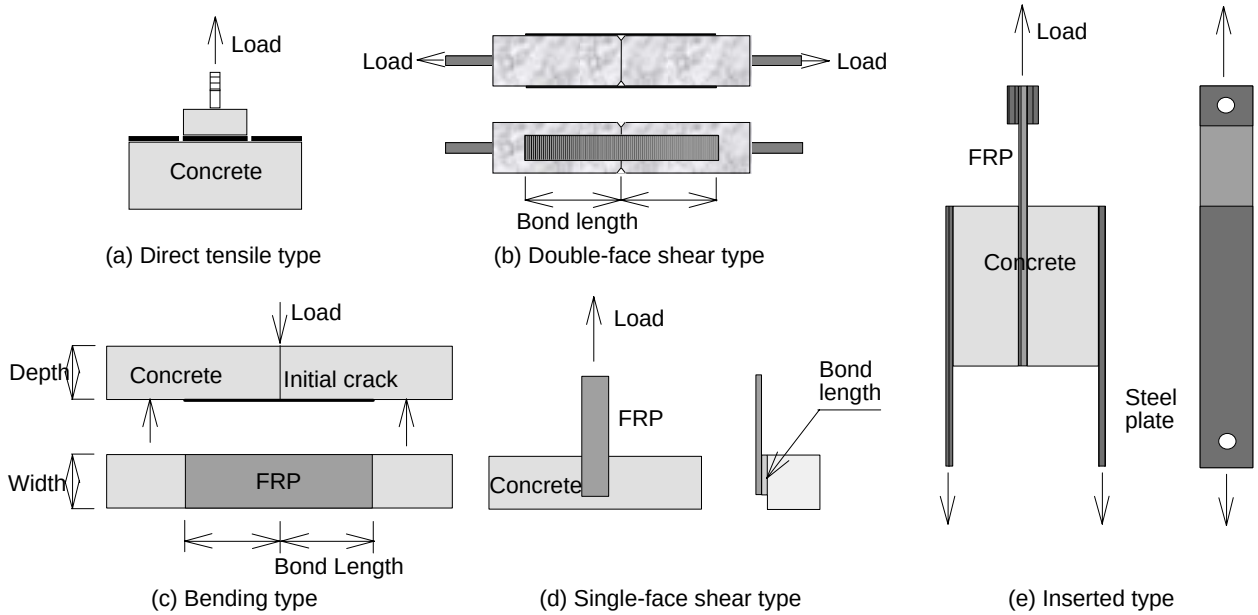

Fig.1-Bond test specimens.

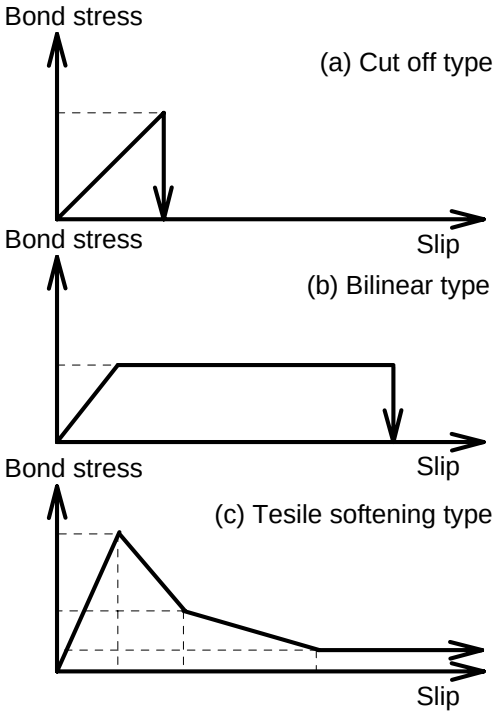

Fig. 2-Bond stress – slip model.

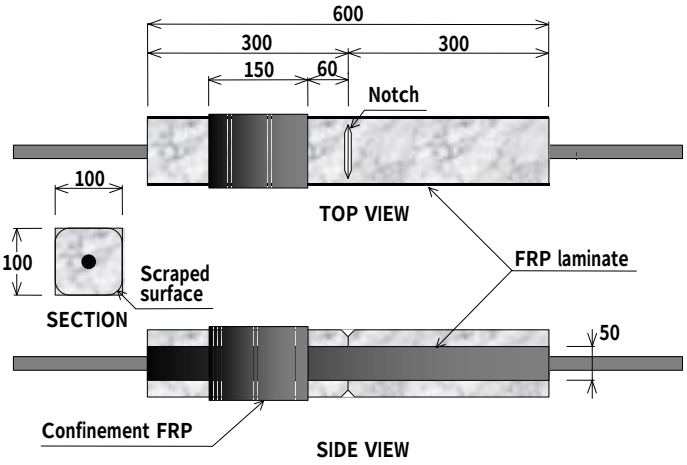

Fig. 3-Test specimen.

crete and mortar. In addition the influence of concrete strength (50 and 24MPa) was verified. The actual strength of the concrete and mortar are shown in Table 2.

Loading and measurements

Each specimen was set in a universal testing machine, and submitted to pure tensile force, causing direct shear to be placed on the laminates. It was not possible, however, to avoid the moment caused by the eccentricity between the top and bottom grips. It will be discussed in greater detail in an upcoming section. The speed used for load application was 1mm/min in the heads speed.

Total displacement and crack width at the center were measured using linear variable displacement transducers (LVDTs), as shown in Fig.5. The strain distribution was obtained from 20 strain gages set on the laminate on one face (the gage face) at intervals of 15mm, and one gage on the opposite sides (the no-gage face), at the center of the specimen.

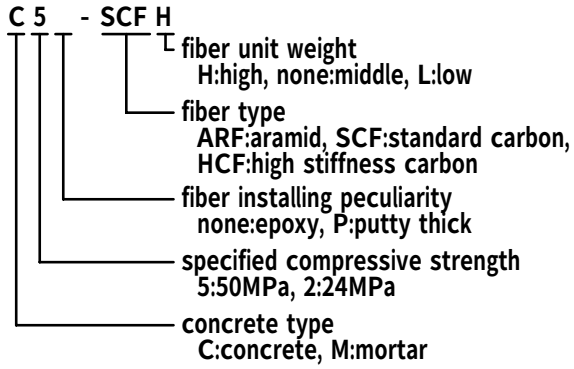

Fig. 4-Identification of the specimen.

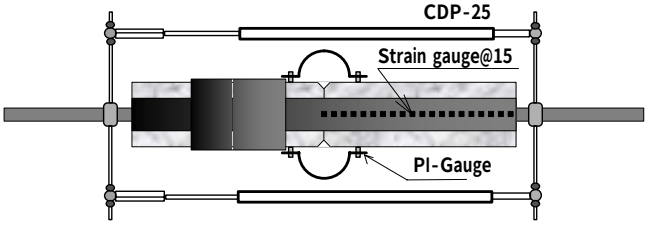

Fig. 5-Data acquisition sketch.

Table 1—Fiber properties

Type of Fiber	Thickness t_f,mm	Unit weight ρ,g/m^2	Tensile strength f_t,MPa	Elastic modulus E_f,MPa
Standard Carbon Fiber	0.167	150/300	4,200	261,100
High Stiffness Carbon Fiber	0.165	300	4,400	425,100
Aramid	0.193	285	2,800	124,500

Table 2—Concrete and mortar properties

Type of Base	Compressive strength σ_B MPa	Splitting strength σ_t MPa	1/3 Secant modulus E_c MPa
Concrete C5	57.6	3.25	29,000
Mortar M5-1	47.1	4.65	24,500
Mortar M5-2	50.9	4.08	25,500
Concrete C2	23.8	1.98	22,000

EXPERIMENTAL RESULTS

Failure detail

All the specimens were submitted to tensile force until total failure of the bond system took place. In the M5 specimens, the substrate surface on the failure face did not present many pieces of mortar bonded on the laminate. Some pieces of concrete on the laminate could be found in the C5 specimens, and a layer of concrete was bonded on the laminate in the C2 specimens after the failure. Typical failure in specimens C2 is shown in Fig.6. These facts are related to the interface between laminates and concrete, which is the region where the epoxy infiltrates into concrete and mortar, and where it is supposed to have a concentrated wearing between FRP and concrete / mortar. The layer of the interface was estimated to have approximately 1 mm for concrete surface[4]. In this research,the interface was not focused, an aspect that may be studied in further research.

Table 3—Test results

Identification of specimen			At max. load		Ultimate		Failure mode
			Load, kN	Displacement, mm	Load kN	Displacement, mm	
C5	C5-SCFH	(1)	51.26	0.824	51.26	0.824	Bond failure on gauge face
		(2)	50.65	0.847	50.65	0.847	Bond failure on no gauge face
		(3)	54.48	0.998	54.48	0.998	Bond failure on no gauge face
	C5-SCF	(1)	37.81	1.020	37.81	1.020	Rupture
		(2)	33.92	1.174	30.48	1.297	Bond failure on no gauge face
		(3)	33.27	1.059	33.14	1.078	Bond failure on no gauge face
	C5-SCFL	(1)	24.39	2.780	23.87	2.981	Bond failure on gauge face
		(2)	23.59	2.782	22.96	2.945	Partial Bond failure with longitudinal rupture on no gage face
		(3)	24.45	2.595	24.45	2.595	Bond failure on gauge face
	C5-HCF	(1)	38.98	1.316	37.75	1.476	Rupture on no gauge face
		(2)	38.95	1.428	38.95	1.428	Bond failure on gauge face and rupture on no gage face
		(3)	32.49	1.399	32.49	1.399	Rupture on no gauge face
	C5-ARF	(1)	25.52	1.764	25.52	1.813	Bond failure on no gauge face
		(2)	25.71	2.597	24.99	3.037	Bond failure on gauge face
		(3)	23.76	1.019	21.77	1.749	Bond failure on gauge face
M5	M5-SCFH	(1)	41.28	0.719	41.28	0.719	Bond failure on gauge face
		(2)	44.57	0.684	44.57	0.684	Bond failure on no gauge face
		(3)	47.14	0.723	46.39	0.803	Bond failure on no gauge face
	M5-SCF	(1)	30.70	0.958	30.49	1.529	Bond failure on no gauge face
		(2)	33.72	1.318	33.72	1.318	Bond failure on no gauge face
		(3)	32.58	1.164	32.58	1.164	Bond failure on gauge face
	M5-SCFL	(1)	17.51	2.140	17.50	2.140	Bond failure on gauge face
		(2)	17.46	2.038	16.12	2.241	Bond failure on no gauge face
		(3)	20.04	2.054	19.98	2.144	Bond failure on gauge face
	M5-HCF	(1)	33.12	1.410	33.12	1.410	Bond failure on no gauge face and rupture on gage face
		(2)	32.50	1.040	32.50	1.040	Bond failure on no gauge face
		(3)	29.28	0.715	29.28	0.715	Bond failure on no gauge face
	M5-ARF	(1)	25.71	2.597	25.14	2.665	Bond failure on gauge face
		(2)	24.35	2.256	23.96	2.297	Bond failure on no gauge face
		(3)	25.42	1.752	23.40	2.010	Bond failure on no gauge face
C2	C2-SCF	(1)	28.18	1.369	27.82	1.644	Bond failure on no gauge face
		(2)	27.74	1.343	25.62	1.606	Bond failure on gauge face
		(3)	30.17	1.800	29.89	2.806	Bond failure on gauge face
	C2P-SCF	(1)	29.08	1.479	28.43	1.512	Bond failure on no gauge face
		(2)	30.28	1.569	29.57	1.616	Bond failure on gauge face
		(3)	30.58	1.046	25.24	1.718	Bond failure on no gauge face

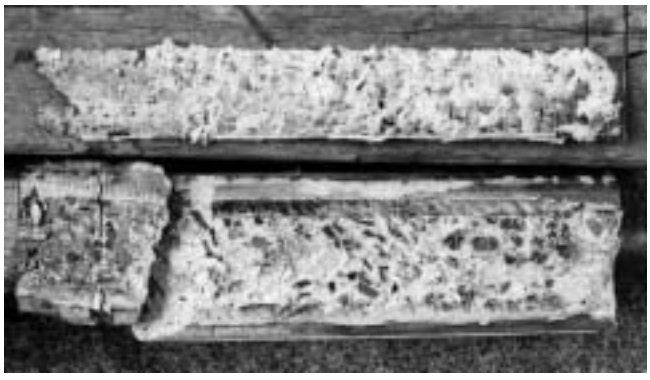

Fig.6-Typical failure surface

Maximum load

Table 3 shows the maximum load, the ultimate load, and the respective displacements of all specimens tested. This table also shows the failure mode and the face where the failure took place. As previously mentioned, gage face herein means the face (side) where the strain gauges were distributed. The opposite, or no-gage, face has only one gage located at the center of the specimen. The specimens were supposed to be under pure tensile force, but it was not possible to avoid the moment caused by the eccentricity between the top and bottom grips when the specimens were set on the loading machine. Due to this, the maximum load was not considered equally distributed in the two laminates. The maximum load in the face where the failure occurred was calculated as follows

$$\text{maximum load at failure face} = \text{maximum load} \times \frac{\text{Strain at failure face}}{(\text{strain at failure face} + \text{strain at no failure face})}$$

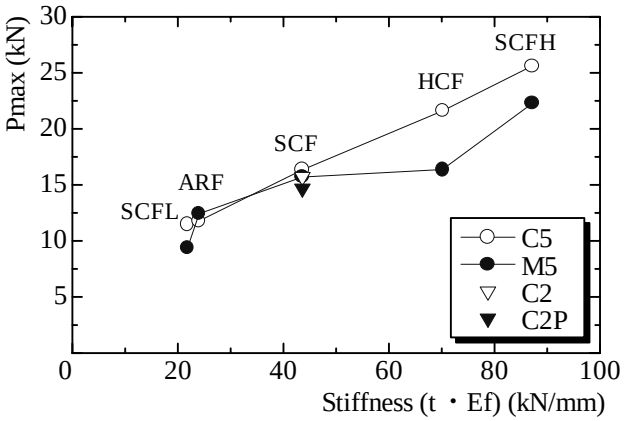

Fig. 7-Maximum load versus stiffness relationship

The strain used is obtained from the strain gages at the center of the specimen in both faces. Table 4 includes the average results of the maximum load at failure face. The specimens that had rupture or partial rupture were not considered for the average calculations

Figure.6 shows the maximum load versus stiffness of the FRP relationship. Each plotted point of the graph consists of a combination of concrete (C5 and C2) or mortar (M5) with FRP (carbon and aramid) stiffness. The stiffness is defined as the thickness multiplied by the elastic modulus of the FRP. It was observed that the maximum load increases as the stiffness of FRP also increases. Specimen C2P-SCF was made to verify the effect of thickness of putty layer (putty layer = 1 mm), but the experimental results of C2-SCF and C2P-SCF did not present a great difference. This means that the thickness of putty had no significant effect on bond behavior.

Load – displacement relationships

The load-displacement graph was plotted using data obtained from the total displacement and crack width. Total displacement is the average between the data at two opposite edges, and the crack width is the average of data from two LVTDs. Examples of these graphs are shown in Fig.8. The behavior of the specimens during the test can be seen with more details in these graphs. The load in specimens using aramid (ARF) and low stiffness carbon fiber (SCFL) becomes constant as it approaches the maximum load, while the displacement continues to grow. On the other hand, SCF, HCF, and SCFH specimens do not allow an excessive elongation before the failure, and thus reach higher maximum loads.

Strain distribution

The data obtained from the strain gages on the laminate was used to create strain versus the distance of the strain gage from the center of the specimen. Figure.9 shows examples of strain distribution of the C5 series. Each curve is a plot of strain at maximum load. The length of the section, where the strain distribution has larger slope, becomes longer as the stiffness of FRP increases. This means that the active bond stress section changes with the stiffness.

LOCAL BOND STRESS - SLIP RELATIONSHIP

Local bond stress

The difference of tensile force is obtained from the strain of Section *i* and the relative strain of preceding Section *i-1*. The average bond stress of section *i*, $\tau_{b,i}$, has been calculated

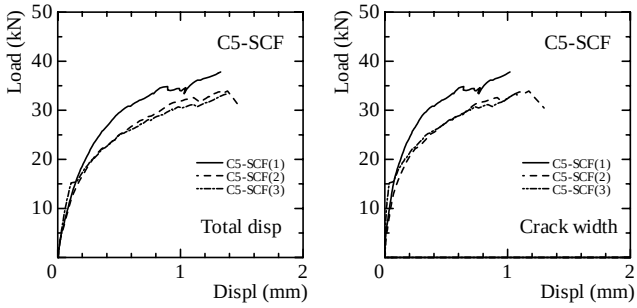

Fig.8- Examples of load - displacement relationship

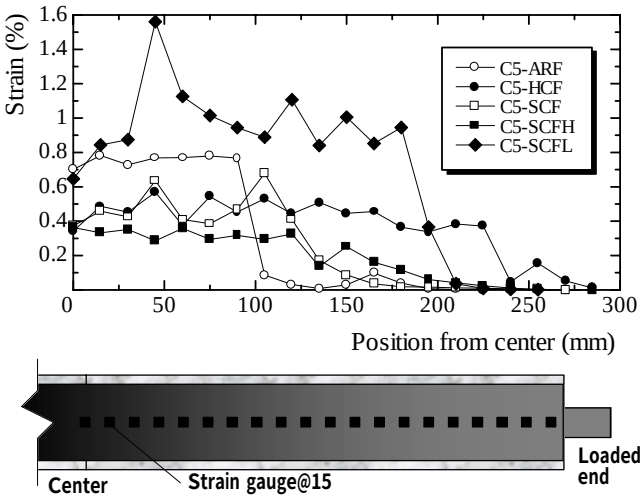

Fig.9-Strain distribution on the laminate in C5 series

dividing the difference of tensile force by the surface area of the laminate, as shown in Eq. (1).

$$\tau_{b,i} = \frac{(\varepsilon_{f,i} - \varepsilon_{f,i-1}) \cdot t_f \cdot E_f}{\Delta l_b} \quad (i = 2 - 20) \tag{1}$$

where,

$\varepsilon_{f,i}$ = strain of FRP of section *i*;
t_f = thickness of FRP;
E_f = elastic modulus of FRP; and
Δl_b = interval between gages (= 15mm).

Slip

The slip of Section *i*, s_i, is the sum of the difference between the elongation of FRP and the elongation of the equivalent section compounded of concrete, epoxy layer and steel bar, from the free end of the laminate (or the loaded end of the specimen) to Section *i*. It is assumed that the relative displacement between concrete and laminate at the free end of the laminate is zero. The slip is calculated using the following equations.

$$s_i = s_{i-1} + (\delta_{f,i} - \delta_{m,i}) \quad (i = 2 - 20, \ s_1 = 0) \tag{2}$$

$$\delta_{f,i} = \frac{\varepsilon_{f,i} - \varepsilon_{f,i-1}}{2} \cdot \Delta l_b + \varepsilon_{f,i-1} \cdot \Delta l_b \tag{3}$$

$$\delta_{m,i} = \frac{\varepsilon_{m,i-1} - \varepsilon_{m,i}}{2} \cdot \Delta l_b + \varepsilon_{m,i} \cdot \Delta l_b \tag{4}$$

Table 4 Maximum load at failure face and fitting results

Specimen	Maximum experimental load ,kN	Stiffness $t_f \cdot E_f$ kN/mm	Maximum bond stress average,MPa	Total average MPa	Slip at maximum bond stress average mm	Total average, mm	n average	Total average	Analytical load , kN
C5-ARF	11.79	24.04	7.173		0.063		3.3		12.56
C5-HCF	21.60	70.14	9.129		0.060		3.3		20.81
C5-SCF	16.35	43.60	7.494	7.583	0.072	0.065	2.5	3.2	16.68
C5-SCFH	25.63	87.19	6.790		0.060		3.7		22.99
C5-SCFL	11.48	21.80	7.328		0.072		3.1		11.99
M5-ARF	12.43	24.04	6.497		0.066		3.2		12.35
M5-HCF	16.37	70.14	7.710		0.046		3.4		20.41
M5-SCF	15.70	43.60	6.253	6.946	0.067	0.060	2.9	3.0	16.37
M5-SCFH	22.29	87.19	6.834		0.063		2.5		22.51
M5-SCFL	9.35	21.80	7.438		0.059		3.3		11.78
C2-SCF	15.71	43.60	6.989		0.052	0.070	3.2	2.9	15.24
							2.7		15.24

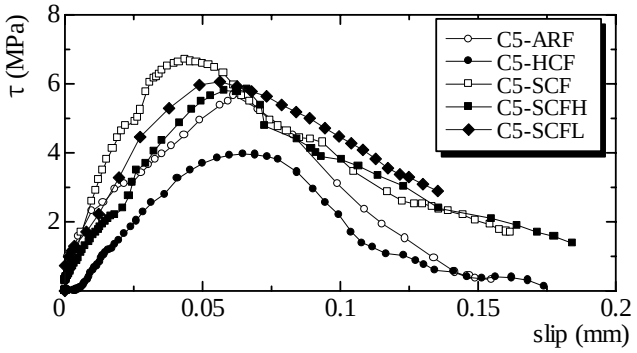

Fig. 10- Measured bond stress vs. slip of C5 series

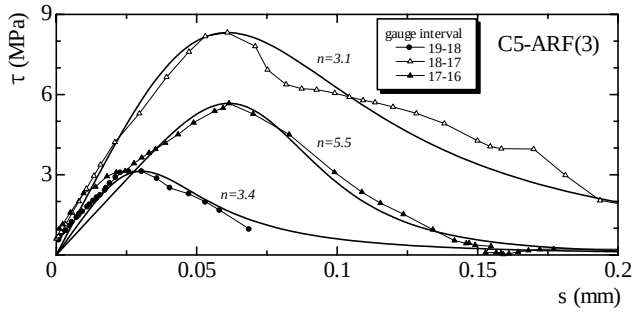

Fig. 11-Fitting results by Popovics equation

$$\varepsilon_{m,i} = \frac{P_{m,i-1} - 2 \cdot \tau_{b,i} \cdot b \cdot \Delta l_b}{A_m \cdot E_m} \qquad (5)$$

$$(\varepsilon_{m,1} = P_{m,1} / A_m \cdot E_m, \quad P_{m,1} = P_{load})$$

where,

$\delta_{f,i}$ = elongation of FRP in Section *i*;

$\delta_{m,i}$ = elongation of equivalent Section *i*;

$\varepsilon_{m,i}$ = strain of equivalent Section *i*;

$P_{m,i}$ = force acting on equivalent Section *i*;

b = width of laminate;

P_{load} = tensile load obtained by loading machine; and

$A_m \cdot E_m$ = stiffness of equivalent section.

After calculating all the data, local bond stress versus slip (τ_b versus *s*) graphs for each gage interval for all specimens were plotted. Figure 10 shows examples of C5 series. These curves have a tendency to become a parabolic in form. The approximation and fitting of a model will be discussed in the following section.

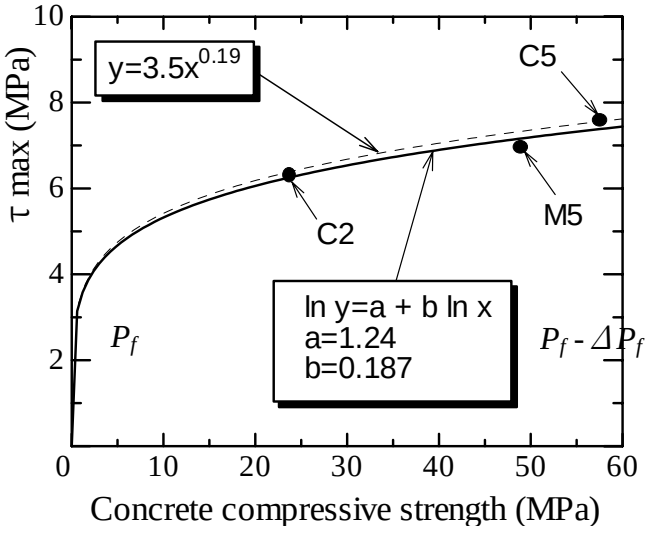

Fig.12-Relationship between maximum bond stress and concrete compressive strength

PROPOSAL OF LOCAL BOND STRESS - SLIP RELATION

Fitting for Popovic's equation

The objective of this research is to present a model that can represent the local bond stress versus slip (τ_b versus *s*) relationship. The formula chosen to calculate the bond stress was Popovics's equation[7], shown as follows

$$\frac{\tau_b}{\tau_{b,\max}} = \frac{s}{s_{\max}} \cdot \frac{n}{(n-1)+(s/s_{\max})^n} \qquad (6)$$

where,

$\tau_{b,\max}$ = maximum local bond stress;

$s_{\max}$ = slip at $\tau_{b,\max}$; and

n = constant.

$\tau_{b,max}$ and s_{max} are obtained directly from the experimental τ_b versus *s* relationship. The value of *n* is calculated by the least square method using normalized τ_b versus *s* relationship. Figure 11 shows graphically some results of Specimen

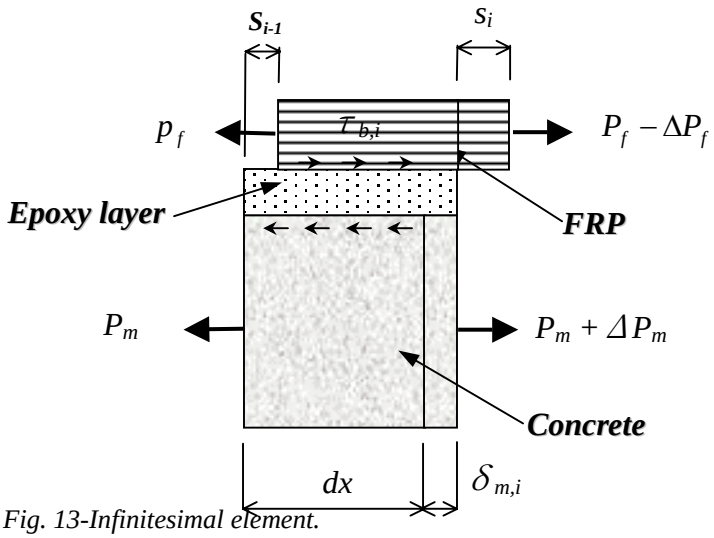

Fig. 13-Infinitesimal element.

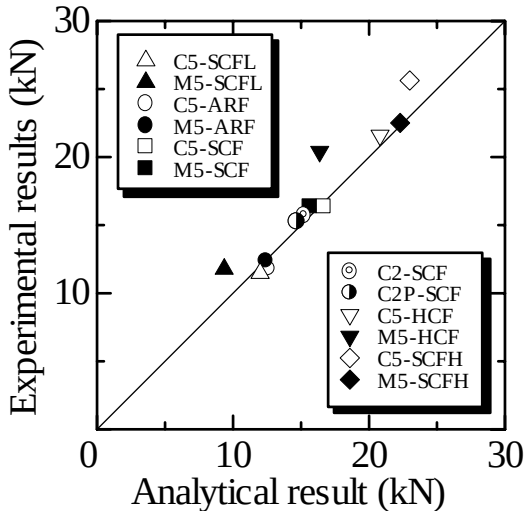

Fig.14-Relationship between experimental maximum load and analytical maximum load.

C5-ARF(3).Table 4 includes the fitting results of the average of three specimen's combination of concrete and mortar-FRP. Maximum local bond stress, $\tau_{b,max}$, ranges from 5.6 to 9.1MPa and slip at $\tau_{b,max}$ ranges from 0.052 to 0.087mm. The constant n is almost 3. Though these values have no clear relationship to FRP type, $\tau_{b,max}$ shows a tendency to increase when the concrete compressive strength increases. The relationship between the maximum bond stress average and the respective concrete/mortar strength was analyzed. The approximation follows equation $\ln y = a + b \ln x$, with a = 1.24 and b = 0.187. The result is $\tau_{b,max} = 3.5 \ \sigma_B^{0.19}$, and is shown in Fig.12. The adopted values of s_{max} and n are the average of the all specimens, shown in Table 4. The final results for Popovics's model are

$$\frac{\tau_b}{\tau_{b,\max}} = \frac{s}{s_{\max}} \cdot \frac{n}{(n-1)+(s/s_{\max})^n} \tag{7}$$

$$\tau_{b,\max} = 3.5\sigma_B^{\ 0.19} \tag{8}$$

where,

τ_b = local bond stress , MPa;

s = slip ,mm:

$\tau_{b,\max}$ = maximum local bond stress, MPa;

Table 5-Effective bond length for each combination concrete/mortar – FRP

Specimen	Effective bond length mm	Stiffness ($t_f \cdot E_f$) ,kN/mm
C5-ARF	65.9	24.04
C5-SCF	95.7	43.60
C5-SCFL	63.5	21.80
C5-SCFH	133.5	87.19
C5-HCF	120.3	70.14
M5-ARF	70.3	24.04
M5-SCF	96.6	43.60
M5-SCFL	67.0	21.80
M5-SCFH	134.1	87.19
M5-HCF	121.2	70.14
C2-SCF	99.1	43.60

$s_{\max}$ = slip at $\tau_{b,\max}$ = 0.065mm;

n = constant = 3; and

σ_B = concrete compressive strength , MPa.

When adapting this model, concrete compressive strength should be kept between 24 and 58 MPa.

ADAPTATION OF PROPOSED MODEL

Method of analysis

To confirm the proposed bond stress-slip relationship, an analytical program was performed. This was done by analyzing the equilibrium of the acting force and the compatibility of deformation at an infinitesimal element, shown in Fig.13. Assuming that the internal bond stress of the element is constant, the slip is obtained from the difference of deformation between laminate and the equivalent section (concrete, epoxy and steel). The bond stress is calculated using the slip, and was obtained by the following sequence:

(i = 2 to n : n is the number of the infinitesimal element)

1.Denominating the slip at free end as s_1;

2.The bond stress of the infinitesimal element i ($\tau_{b,i}$) is calculated using the slip at section i-1 (s_{i-1}) on the model;

3.The increment of force $\Delta P_{f,i}$, the elongation of the laminate $\delta_{f,i}$, and the elongation of the equivalent section, $\delta_{m,i}$ of the infinitesimal element i are calculated using the following equations

$$\Delta P_{f,i} = \tau_{b,i} \cdot b \cdot \Delta x \tag{9}$$

$$\delta_{f,i} = \frac{\Delta x}{t_f \cdot b \cdot E_f}\left(\sum_{k=1}^{i-1} \Delta P_{f,k} + \frac{\Delta P_{f,i}}{2}\right) \tag{10}$$

$$\delta_{m,i} = \frac{\Delta x}{A_m \cdot E_m}\left(\sum_{k=i+1}^{n} \Delta P_{m,k} + \frac{\Delta P_{f,i}}{2}\right) \tag{11}$$

4.Calculation of slip s_i, tensile load $P_{f,i}$, and FRP strain $\varepsilon_{f,i}$ using the next equations

$$s_i = s_{i-1} + (\delta_{f,i} - \delta_{m,i}) \tag{12}$$

$$P_{f,i} = P_{f,i-1} + \Delta P_{f,i} \tag{13}$$

Table 6—Parameters of Kamiharako et al. experiment

	Concrete		FRP					
Specimen	Compressive strength ,MPa	Elastic modulus, MPa	Fiber type	Thickness, mm	Elastic modulus ,GPa	Width ,mm	Length ,mm	Failure mode
S1-1	34.9	27500	Carbon	0.111	270	10	145	Fiber rupture
S1-2	36.3	28000				10	250	Fiber rupture
S1-3	36.3	28000				20	145	Fiber rupture
S1-4	36.3	28000				20	175	Bond failure
S1-5	34.9	27500				30	100	Bond failure
S1-6	34.9	27500				30	175	Fiber rupture
S1-7	38.8	29000				30	250	Bond failure
S1-8	36.3	28000				50	250	Fiber rupture
S1-9	41.5	30000				70	175	Bond failure
S1-10	41.5	30000				90	175	Bond failure
S2-1	38.8	29000	Aramid	0.169	80	30	175	Bond failure
S2-2	36.5	28100				30	200	Bond failure
S3-1	42.4	30300	Carbon	0.111	270	30	175	Fiber rupture
S3-2	36.5	28100	Aramid	0.169	80	30	200	Bond failure
S4-1	35.1	27600	Carbon	0.222	270	30	175	Bond failure
S5-1	**53.4**	**34000**	**Carbon**	**0.111**	**270**	**30**	**175**	**Fiber rupture**
S5-2	**75.5**	**40400**				**30**	**175**	**Bond failure**
S6-1	**42.4**	**30300**				**30**	**175**	**Bond failure**

Table7- Analytical results using Kamiharako et al. parameters

Specimen	Maximum load average from experiment ,kN	Maximum load from analysis ,kN	Comparison exp/ana
S1-1	6.25	5.31	1.18
S1-2	5.78	5.45	1.06
S1-3	9.84	10.57	0.93
S1-4	8.78	10.67	0.82
S1-5	12.89	15.17	0.85
S1-6	14.71	15.75	0.93
S1-7	12.83	16.12	0.80
S1-8	22.52	26.11	0.86
S1-9	29.84	35.84	0.83
S1-10	29.38	45.21	0.65

$$\varepsilon_{f,i} = \frac{P_{f,i}}{t_f \cdot b \cdot E_f} \quad (14)$$

5. The bond stress calculation is repeated from the infinitesimal slip of the free end to the step where the bond stress becomes extremely small.

The tensile load acting on the laminate is $P_{f,n}$, and the Δx adopted is 0.1mm.

Comparison between analytical results and experimentalExperimental results

The proposed model was adapted and verified using the next graph Fig.14. Fig.14 shows the comparison between experimental and analytical results of the maximum load. It can be seen that the analytical results represent very well the experimental results.

Effective bond length

The bond stress is distributed in a limited area of the laminate, and the load is sustained in the vicinity of the loading point. When the delamination of the laminate occurs due to the fracture of concrete, the active bonding area shifts to a new area, and it continues until the delamination propagates completely.It is assumed that when the bond stress reaches a maximum level,it keeps the form and moves to the free end of the laminate.

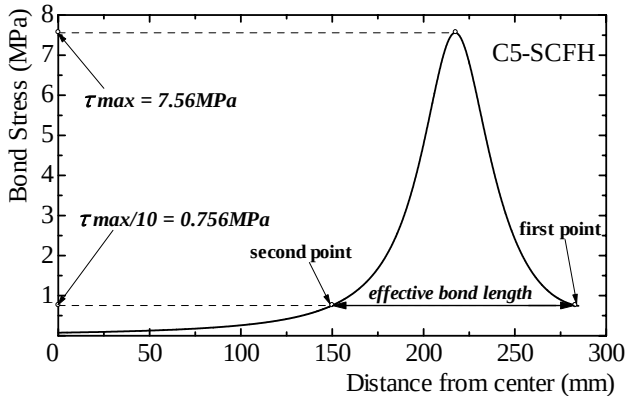

Fig.15-Example of effective bond length.

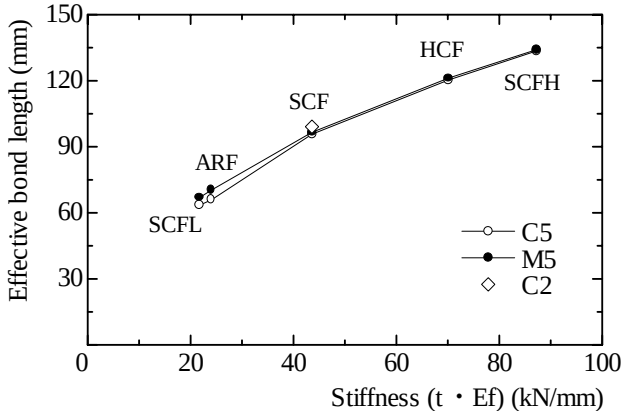

Fig.16-Effective bond strength versus stiffness.

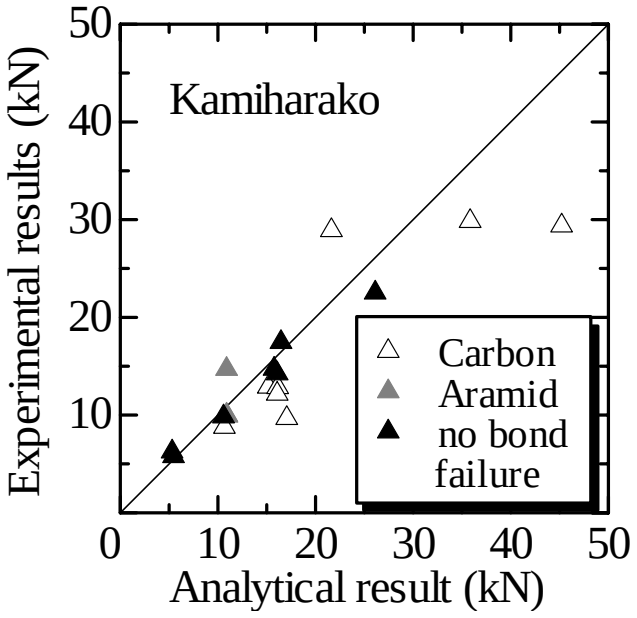

Fig. 17-Results from Kamiharako et al.

It is also determined herein that the effective bond length is the distance between two points that correspond to 10% of the maximum bond stress. Fig.15 shows graphically the effective bond length. The effective bond length for each combination concrete / mortar - FRP are shown in Table5. It can be seen that the effective bond length is related to the stiffness of FRP. Table 5 is graphically represented in Fig.16.

Comparison with previous study

To verify the validity of this model, the maximum load was calculated by the model proposed in this research using data from Kamiharako's previous study[6], and was compared with the experimental results. The experiment had used the same specimen with a cross section of 100 x 100mm. The parameters are: concrete strength, type of fiber (carbon and aramid), width and length of laminate, layer of laminates, and elastic modulus of resin. The parameters are shown in Table 6 and the results are shown in Table7. The results are represented graphically in Fig.17. Analytical strengths show good correspondence with the experimental strengths for most specimens. The ratio of experimental values to analysis becomes smaller, when the width of laminates becomes larger. It is supposed that failure other than bond delamination took place when the width of the laminates was almost same as the width of specimen.

CONCLUSIONS

In this research, a local bond stress – slip model was proposed based on Popovics's equation, which represents with good accuracy the experimental results. The model was also verified by comparing the test results from a previous study with the analytical results obtained with the present model. Additionally, the effective bond length for each combination of FRP – concrete / mortar was presented. The following conclusions can be made from this experiment:

1.The maximum load increases as the stiffness of FRP also increases;

2.Putty thickness is shown to have no affect, and the incremental increase of its layer did not imply an increase in maximum load; and

3.Maximum local bond stress is not influenced by the type of FRP, but increases as concrete compressive strength increases.

ACKNOWLEDGEMENTS

The financial assistance provided by University of Tsukuba Project is gratefully acknowledged.

NOTATIONS

$A_m \cdot E_m$	=	stiffness of equivalent section
b	=	width of laminate
E_f	=	elastic modulus of FRP
n	=	constant for Popovics's equation
$P_{f,i}$	=	force acting on FRP Section *i*
P_{load}	=	tensile load obtained by loading machine
$P_{m,i}$	=	force acting on equivalent Section *i*
s	=	slip
$s_{\max}$	=	slip at $\tau_{b,\max}$
t_f	=	thickness of FRP
Δl_b	=	interval between gages
$\Delta P_{f,i}$	=	increment of acting force of FRP in Section *i*
$\Delta P_{m,i}$	=	increment of acting force of equivalent Section *i*
Δx	=	length of infinitesimal element
$\delta_{f,i}$	=	elongation of FRP in Section *i*
$\delta_{m,i}$	=	elongation of equivalent Section *i*
$\varepsilon_{f,i}$	=	strain of FRP of Section *i*
$\varepsilon_{m,i}$	=	strain of equivalent Section *i*
σ_B	=	concrete compressive strength
τ_b	=	local bond stress
$\tau_{b,\max}$	=	maximum local bond stress

REFERENCES

1.Horiguchi, T. and Saeki, N., "Effect Test Method and Quality of Concrete on Bond Strength of CFRP Sheet,"*Proceedings of Third International Symposium of Non-Metallic (FRP) Reinforcement for Concrete Structures*, Vol. 1, 1997, pp. 265-270.

2.Okano, M.; Ohuchi, H.; Moriyama, T.; Matsumoto, N.; and Wakui, H., "Carbon Fiber Retrofit of Railway Viaducts Columns, " *Proceedings of Third International Symposium of Non-Metallic (FRP) Reinforcement for Concrete Structures*, Vol. 1, 1997, pp. 403-410.

3.Maeda, T.; Asano, Y.; Sato, Y.; Ueda, T.; and Kakuta, Y., "A Study on Bond Mechanism of Carbon Fiber Sheet, " *Proceedings of Third International Symposium of Non-Metallic (FRP) Reinforcement for Concrete Structures*, Vol. 1, 1997, pp. 279-286.

4.Sato, Y.; Kimura, K. and Kobatake, Y., "Bond Behavior between CFRP Sheet and Concrete (Part 1), " *Journal of Structural and Construction Engineering*, Architectural Institute of Japan, Vol. 500, 1997, pp. 75-82 (in Japanese).

5.Brosens K. and Van Gemert D. "Anchorage Design for Externally Bonded Carbon Fiber Reinforced Polymer Laminates", *Fiber Reinforced Polymer Reinforcement for Concrete Structures*, American Concrete Institute, Frmington Hills, Mich., 1999, pp. 635-645.

6.Kamiharako, A., Shimomura, T., Maruyama, K. and Nishida, H., "Analysis of Bond and Debonding Behavior of Continuous Fiber Sheet Bonded on Concrete", *Journal of Materials, Concrete Structures and Pavements*, Japan Society of Civil Engineers, Vol. 634, 1999, pp. 197-208. (in Japanese)

7.Popovics,S."A Numerical Approach to Complete Stress-StrainCurve of Concrete", *Cement and Concrete Research*, Vol. 3, 1973, pp. 583-559.